

Plastic characterization of metals by combining nanoindentation test and finite element simulation

Yong MA¹, Ying ZHANG¹, Hai-feng YU¹, Xiang-yu ZHANG¹, Xue-feng SHU², Bin TANG¹

1. Research Institute of Surface Engineering, Taiyuan University of Technology, Taiyuan 030024, China;

2. Research Institute of Applied Mechanics and Biomedical Engineering,
Taiyuan University of Technology, Taiyuan 030024, China

Received 18 June 2012; accepted 16 October 2012

Abstract: Materials with the same elastic modulus E and representative stress and strain (σ_r , ε_r) present similar indentation–loading curves, whatever the value of strain hardening exponent n . Based on this definition, a good approach was proposed to extract the plastic properties or constitutive equations of metals from nanoindentation test combining finite element simulation. Firstly, without consideration of strain hardening, the representative stress was determined by varying assumed representative stress over a wide range until a good agreement was reached between the computed and experimental loading curves. Similarly, the corresponding representative strain was determined with different hypothetical values of strain hardening exponent in the range of 0–0.6. Through modulating assumed strain hardening exponent values to make the computed unloading curve coincide with that of the experiment, the real strain hardening exponent was acquired. Once the strain hardening exponent was determined, the initial yield stress σ_y of metals could be obtained by the power law constitution. The validity of the proposed methodology was verified by three real metals: AISI 304 steel, Fe and Al alloy.

Key words: nanoindentation; finite element simulation; representative stress; representative strain; initial yield stress

1 Introduction

Nanoindentation, originally developed by DOERNER and NIX [1] and later further improved by OLIVER and PHARR [2,3], is arguably one of the quickest and simplest ways of measuring the mechanical properties of materials, such as hardness and elastic modulus, at the micro, submicro, and nanoscales [4–8]. In recent years, interest has been mounting in the development of extracting the constitutive equations of engineering metals from nanoindentation [9,10]. However, the analysis of nanoindentation response to obtain the plastic properties of elastoplastic metals is not an easy task. Sometimes application of the concept of representative strain can significantly simplify the analysis of the nanoindentation response and is also the main concern of the present work. The concept of representative strain was first introduced by TABOR [11], who pointed out that hardness was proportional to

uniaxial stress in large domain, at a representative plastic strain of 0.082. Through finite element and dimensionless analysis of nanoindentation, DAO et al [12] redefined the representative strain, 0.033 for Berkovich indenter. Noticing the limitation of the representative strain defined by DAO et al, other definitions and/or values of representative strain were proposed. ANTUNES et al [13] concluded that representative strain ranged from 0.034 to 0.042 depending on the ratio of reduced modulus E_r and representative stress (corresponding representative strain). OGASAWARA et al [14] presented a representative strain definition with the physical basis, and the value was 0.0115 for Berkovich indenter. Through further investigation, CAO and HUBER [15] proposed several other definitions. The publications have to be considered as indicative, since a larger number of related ones are dealing with the same subjects.

So far, however, there is not a robust way to determine the representative strain and corresponding

stress. Therefore, a general approach to determine the plastic properties of metals with the application of representative stress and strain has not been established. Based on the results of aforementioned authors, the aim of this work is to present a good method only by using numerical simulations to determine the plastic properties or power law constitutive equations of metals. Considering that materials with the same elastic modulus and representative stress and strain values present similar indentation–loading curves, whatever the value of the strain hardening exponent [12], the representative stress was firstly determined without consideration of strain hardening. Then, the representative strain was determined with different hypothetical values of n in a range from 0.1 to 0.6. Finally, the strain hardening exponent and initial yield stress were obtained through comparing the unloading curves of nanoindentation test and finite element simulation.

The whole procedure of analysis was carried out on an assumed metal with $E=419$ GPa, $\sigma_y=6.5$ GPa and $n=0.3$. Considering the generality, all the above mechanical parameters were selected randomly. The forward analysis [12] results were considered as experimental results. In order to verify the validity of this methodology, it was applied to three real metals at last.

2 Finite element simulation of nano-indentation

During nanoindentation measurement, a sharp rigid indenter penetrates normally into a homogeneous solid where the indentation load P and displacement h are continuously registered in one complete loading–unloading cycle (Fig. 1). During loading, the response generally follows the relation described by Kick’s Law:

$$P=Ch^2 \tag{1}$$

where C is the loading curvature, which can be obtained by curve fitting.

The maximum indentation depth h_{max} occurs at the maximum load P_{max} . The initial unloading slope (contact stiffness) is

$$S = \left(\frac{dP_u}{dh} \right)_{h=h_{max}} \tag{2}$$

where P_u is the unloading load.

When the maximum load is removed (relaxation stage), owing to the resulting material plastic deformation, there is a remaining depth h_r . W_t is the total work under the loading curve, which includes the elastic recovery work W_e and the residual plastic work W_p .

An axisymmetric finite element model of the semi-infinite space is developed to simulate nanoindentation

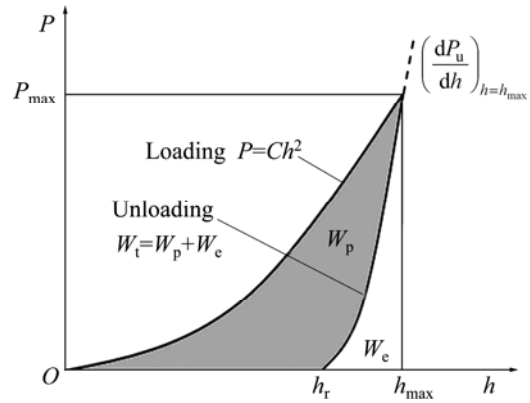


Fig. 1 Typical P – h curve of an elastoplastic material to instrumented sharp nanoindentation

test, as demonstrated in Fig. 2. The pyramid shaped indenter is treated the same as conical indenter with a cone angle of 70.3° providing the same area to depth relationship. Metal materials are modeled using 4 node axisymmetric reduced integration elements while the indenter is modeled as a rigid element. Surface-to-surface contact elements are applied to the exposed surfaces for which there are a possibility of touching each other. The friction between the tip and the specimen surface is assumed to be 0.16 [13]. The horizontal displacement is fixed on symmetric boundaries, and the vertical displacement is fixed on the model bottom. Metals are assumed to be homogeneous and isotropic. The static analysis including the large deflection is carried out using the commercial finite element package ANSYS v.10.0. The power law form (Fig. 3) of metals constitutive equation is expressed as

$$\sigma = \begin{cases} E\varepsilon, & \sigma \leq \sigma_y \\ R\varepsilon^n = \sigma_y \left(1 + \frac{E}{\sigma_y} \varepsilon_p \right)^n, & \sigma > \sigma_y \end{cases} \tag{3}$$

where ε_p is nonlinear part of the total effective strain that is great than ε_y ($=\sigma_y/E$).

The representative strain ε_r is defined to be the plastic strain, i.e., for uniaxial loading:

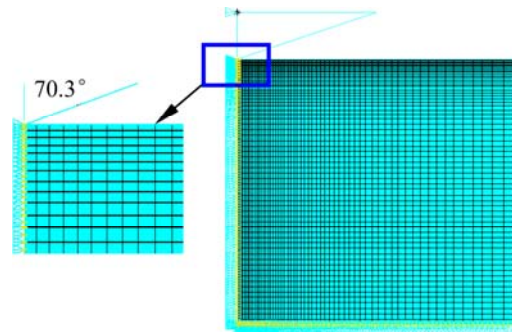


Fig. 2 Model geometry used in indentation finite element simulation

$$\varepsilon = \varepsilon_e + \varepsilon_p \equiv \varepsilon_e + \varepsilon_r \quad (4)$$

Therefore, the corresponding representative stress is

$$\sigma_r = \sigma_y \left[\frac{E}{\sigma_y} \left(\frac{\sigma_r}{E} + \varepsilon_r \right) \right]^n \quad (5)$$

To complete the material constitutive description, Poisson's ratio ν is assumed to be 0.3, and the incremental theory of plasticity with von Mises equivalent stress (J_2 flow theory) is proposed.

3 Determining plastic properties of metals

3.1 Extracting representative stress and strain

Using the hardness H and the reduced modulus E_r of materials, σ_r is estimated [13]. The relation is linearly expressed as

$$\frac{E_r}{H} = 0.231 \left(\frac{E_r}{\sigma_r} \right) + 4.91 \quad (6)$$

With the same definition of this work, CAO and HUBER [15] described ε_r as the function of C/E_r instead of a constant [16]:

$$\varepsilon_r = 0.04734 - \frac{0.02466}{\left(1 + \exp\left(\frac{C/E_r - 0.6772}{0.21139} \right) \right)} \quad (7)$$

In this work, the two equations are firstly used to initially estimate the values of representative stress and strain, and then numerical simulations are implemented to refine them. The refining performance does not end until simulated and experimental results have a good agreement.

As discussed above, the indentation loading curves of materials with the same E and $(\sigma_r, \varepsilon_r)$ values are independent of the strain hardening exponent. Adopting the special case of $n=0$, as shown in Fig. 3, the representative stress can be determined by comparing the experimental and numerical loading curves until a good agreement is reached. Figure 4 indicates that the numerical loading curve agrees well with the experimental loading curve when the representative plastic stress equals 9.655 GPa. The relative error of F_{\max} (experimental, Exp) and F_{\max} (finite element methods, FEM) is less than 0.15%.

Considering different assumed values of strain hardening exponent, as shown in Fig. 3, the value of the representative strain is similarly determined by the comparison of the simulated and experimental loading curves. Figure 5(a) shows that the computed and experimental loading curves are consistent when $\varepsilon_r=0.038$. The relative error of F_{\max} (Exp) and F_{\max} (FEM) is less than 0.12%. Figure 5(b) is the close-up

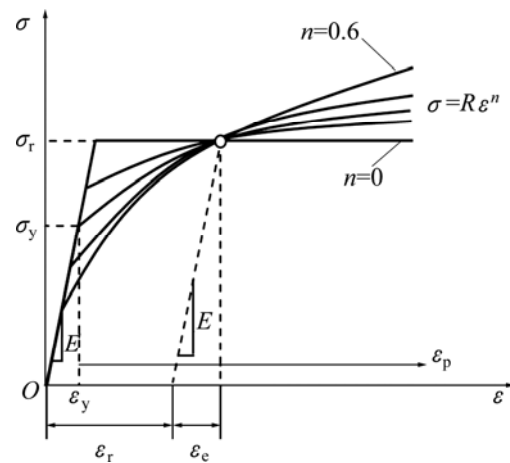


Fig. 3 A schematic diagram of power law stress–strain behavior of metals used in this work

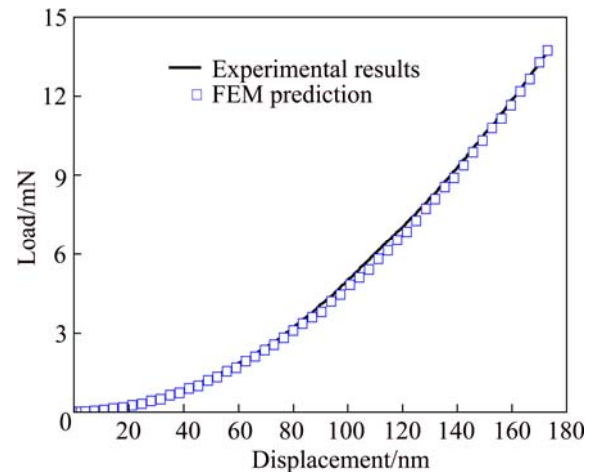


Fig. 4 Simulated and experimental loading curves for assumed metal

view of the final unloading part, which shows that the unloading curves are affected by strain hardening. To be precise, elastic recovery increases slowly along with the increase of the strain hardening exponent. According to the experimental unloading curve, we can conclude that the strain hardening exponent of the assumed metal is between 0.22 and 0.32.

3.2 Extracting strain hardening exponent and initial yield stress

In this section, modificatory simulations are also used to acquire the strain hardening exponent. Finite element simulation begins with the strain hardening exponent $n=0.24$ within the range of 0.22–0.32, and the corresponding initial yield stress σ_y is 7.102 GPa. After a series of modificatory simulations, the simulated and experimental unloading curves achieve a good agreement when $n=0.293$ (Fig. 6). Substituting the values of $(\sigma_r, \varepsilon_r)$ and n into Eq. (5), the precise numerical solution of the

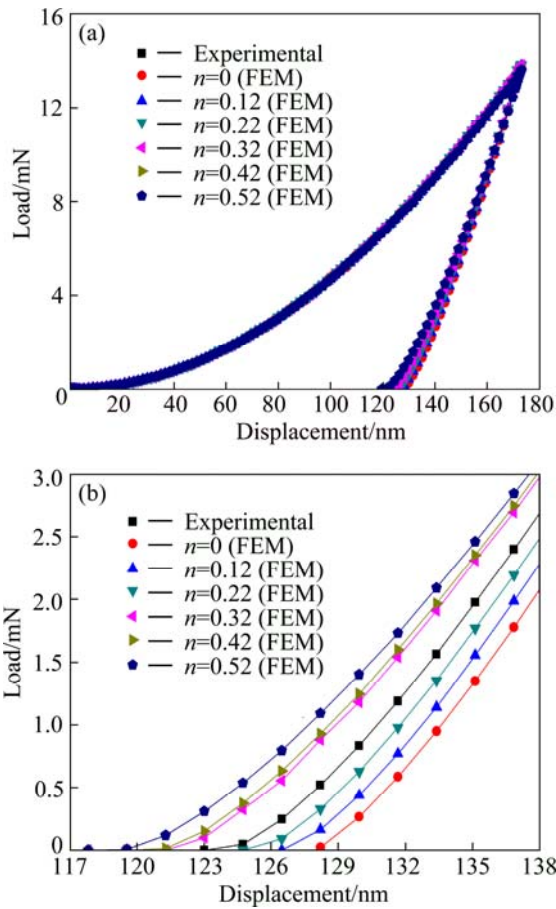


Fig. 5 Load–displacement curves from finite element simulation and experimental results for assumed metal with different assumed values of n : (a) Whole loading–unloading curves; (b) Amplificatory final unloading segments

initial yield stress is finally determined, which is 6.43 GPa. The relative error between σ_y (Exp) and σ_y (FEM) is -1.07% . In the light of the calculation process, it can be concluded that the plastic parameters of metals can be uniquely and precisely determined when the simulated load– displacement curves agree well with those of experiment.

4 Application and discussion

The previously described approach of extracting plastic properties or constitutive equations of the metals

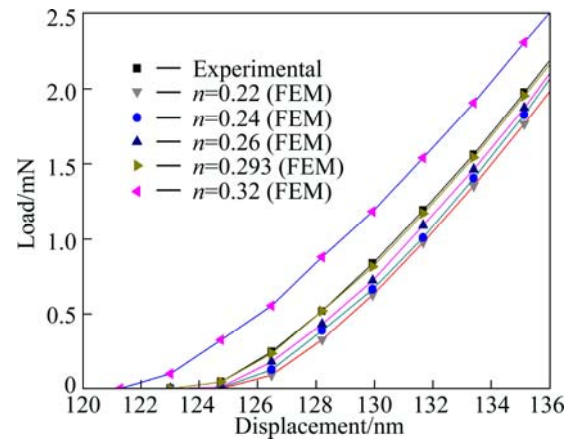


Fig. 6 Experimental and simulated final unloading segments with assumed values of n in range of 0.22–0.32

is applied to three real metals: AISI 304 steel, Fe and Al alloy. Firstly, three metals are tested by ASTM standard tensile instrument and Nano Indenter G200. Tensile tests are conducted with tensile strain rate of 10^{-3} s^{-1} . The tensile test results are listed in Table 1. Nanoindentation tests are performed with indentation depth of 2000 nm which is deep enough to reduce the effects of material surface roughness and size. The nanoindentation test and FEM analysis results are also listed in Table 1. From the comparison of the tensile test results and those of nanoindentation test combining FEM analysis, it can be found that the methodology of this work also possesses practical effectiveness apart from aforementioned uniqueness and preciousness.

In comparison with other methods, the present methodology of this work is feasible and easily performable in practice. PELLETIER et al [17,18] pointed out the limits of using bilinear stress–strain curve for finite element modeling of nanoindentation response on bulk materials and constructed a predictive model to estimate it. Although the bilinear constitutive relationship is a simple model which only contains two unknown parameters, i.e., initial yield stress σ_y and tangent modulus E_t , the calculation method is not easy to implement because of the non-uniqueness. CAO et al [15,19] and OGASAWARA et al [16,20] argued that their methods which were in some extent contrary could both

Table 1 Elastoplastic properties of three real metals obtained by two different methods

Elastoplastic property	Tensile test			Nanoindentation and FEM		
	AISI 304 steel	Fe	Al alloy	AISI 304 steel	Fe	Al alloy
E/GPa	205.60	184.20	78.00	211.50	180.45	79.30
H/GPa	—	—	—	3.40	2.54	1.98
σ_r/GPa	—	—	—	0.725	0.662	0.616
ε_r	—	—	—	0.0206	0.0345	0.0287
σ_y/GPa	0.24	0.32	0.50	0.238	0.316	0.503
n	0.37	0.24	0.12	0.364	0.237	0.116

uniquely and precisely determine the plastic properties of metals, but their algorithms are also difficult to use in practice. Besides the complication of performing calculation, many errors exist in calculating the values of C , S , W_e and W_p (Fig. 1). One alternative method that may solve this problem is to build effective calculation software, which has been carried out by BOUZAKIS and MICHAILIDIS [21,22] and is still being improved.

There are two influencing factors in our methodology. One is the experimental precision; hence, to apply the current method, one must guarantee it firstly. The other is the calculation errors in numerical simulations, which can be limited by modificatory simulations.

5 Conclusions

In this work, nanoindentation test matching finite element simulation was used to characterize the plastic properties or constitutive equations of metals. The representative strain equal to the plastic strain was adopted. The uniqueness and accuracy of this methodology were ensured when calculated and experimental load–displacement curves got a good agreement by gradually modulating finite element simulation parameters. The validity of this methodology was checked by applying it to three real metals. Compared to similar methods, the approach of this work is feasible and can be easily used in practice. Nanoindentation test is the basis of the present work. Therefore, the experiment precision must be guaranteed when it is used.

References

- [1] DOENER M F, NIX W D. A method for interpreting the data from depth-sensing indentation instruments [J]. *Journal of Material Research*, 1986, 1(4): 601–609.
- [2] OLIVER W C, PHARR G M. An improved technique for determining hardness and elastic modulus using load and displacement sensing indentation experiments [J]. *Journal of Material Research*, 1992, 7: 1564–1583.
- [3] PHARR G M, OLIVER W C, BROTZEN F R. On the generality of the relationship among contact stiffness, contact area, and elastic modulus during indentation [J]. *Journal of Materials Research*, 1992, 7: 613–617.
- [4] PHARR G M. Measurement of mechanical properties by ultra-low load indentation [J]. *Materials Science and Engineering A*, 1998, 253(1–2): 151–159.
- [5] FOUGERE G E, RIESTER L, FERBER M, WEERTMAN J R, SIEGEL R W. Young's modulus of nanocrystalline Fe measured by nanoindentation [J]. *Materials Science and Engineering A*, 1995, 204(1–2): 1–6.
- [6] RANDALL N X, CHRISTOPH R, DROZ S, JULIA-SCHMUTZ C. Localised micro-hardness measurements with a combined scanning force microscope/nanoindentation system [J]. *Thin Solid Films*, 1996, 290–291: 348–354.
- [7] MANTE F K, BARAN G R, LUCAS B. Nanoindentation studies of titanium single crystals [J]. *Biomaterials*, 1999, 20(11): 1051–1055.
- [8] AHN J H, KWON D. Micromechanical estimation of composite hardness using nanoindentation technique for thin-film coated system [J]. *Materials Science and Engineering A*, 2000, 285(1–2): 172–179.
- [9] GIANNAKOPOULOS A E, SURESH S. Determination of elastoplastic properties by instrumented sharp indentation [J]. *Scripta Materialia*, 1999, 40(10): 1191–1198.
- [10] CHENG Y T, CHENG C M. Scaling relationships in conical indentation of elastic-perfectly plastic solids [J]. *International Journal of Solids and Structures*, 1999, 36(8): 1231–1243.
- [11] TABOR D. *The hardness of metals* [M]. Oxford: Oxford University Press, 1951: 100–126.
- [12] DAO M, CHOLLACOOP N, VAN VLIET K J, VENKATESH T A, SURESH S. Computational modeling of the forward and reverse problems in instrumented sharp indentation [J]. *Acta Materialia*, 2001, 49(19): 3899–3918.
- [13] ANTUNES J M, FERNANDES J V, MENEZES L F, CHAPARRO B M. A new approach for reverse analyses in depth-sensing indentation using numerical simulation [J]. *Acta Materialia*, 2007, 55(1): 69–81.
- [14] OGASAWARA N, CHIBA N, CHEN X. Measuring the plastic properties of bulk materials by single indentation test [J]. *Scripta Materialia*, 2006, 54(1): 65–70.
- [15] CAO Y P, HUBER N. Further investigation on the definition of the representative strain in conical indentation [J]. *Journal of Materials Research*, 2006, 21: 1810–1821.
- [16] OGASAWARA N, CHIBA N, CHEN X. A simple framework of spherical indentation for measuring elastoplastic properties [J]. *Mechanics of Materials*, 2009, 41(9): 1025–1033.
- [17] PELLETIER H, KRIER J, CORNET A, MILLE P. Limits of using bilinear stress–strain curve for finite element modeling of nanoindentation response on bulk materials [J]. *Thin Solid Films*, 2000, 379(1–2): 147–155.
- [18] PELLETIER H. Predictive model to estimate the stress–strain curves of bulk metals using nanoindentation [J]. *Tribology International*, 2006, 39(7): 593–606.
- [19] CAO Y P, QIAN X Q, LU J, YAO Z H. An energy-based method to extract plastic properties of metal materials from conical indentation tests [J]. *Journal of Materials Research*, 2005, 20: 1194–1206.
- [20] OGASAWARA N, CHIBA N, ZHAO M H, CHEN X. Comments on “Further investigation on the definition of the representative strain in conical indentation” by Y. Cao and N. Huber [J. Mater. Res. 21, 1810 (2006)]: A systematic study on applying the representative strains to extract plastic properties through one conical indentation test [J]. *Journal of Materials Research*, 2007, 22: 858–868.
- [21] BOUZAKIS K D, MICHAILIDIS N. Coating elastic-plastic properties determined by means of nanoindentations and FEM-supported evaluation algorithms [J]. *Thin Solid Films*, 2004, 469–470: 227–232.
- [22] BOUZAKIS K D, MICHAILIDIS N. An accurate and fast approach for determining materials stress–strain curves by nanoindentation and its FEM-based simulation [J]. *Materials Characterization*, 2006, 56(2): 147–157.

纳米压入结合有限元模拟确定金属材料的塑性性能

马永¹, 张莹¹, 于海峰¹, 张翔宇¹, 树学峰², 唐宾¹

1. 太原理工大学 表面工程研究所, 太原 030024;

2. 太原理工大学 应用力学与生物医学工程研究所, 太原 030024

摘要: 材料具有相同的弹性模量 E 以及代表性应力与代表性应变 (σ_r, ε_r) 时, 可以获得相同的纳米压痕加载曲线, 而与材料的应变强化指数 n 无关。基于此, 利用纳米压入结合有限元数值模拟建立一种确定金属材料塑性性能参数的改进方法。首先, 不考虑金属材料的加工硬化, 通过不断调整代表性应力的假设值, 当模拟与实验载荷-位移曲线的加载阶段相吻合时, 确定其代表性应力。其次, 对金属材料假设不同的应变强化指数, 采用相同的方法确定其代表性应变。最后, 通过调整应变强化指数的假设值, 使模拟曲线与实验曲线的卸载阶段相吻合来确定金属材料的真实应变强化指数, 继而利用幂强化本构方程确定金属材料的初始屈服极限。将该方法应用于 AISI 304 不锈钢、铁及铝合金三种金属, 其有效性得到验证。

关键词: 纳米压入; 有限元模拟; 代表性应力; 代表性应变; 初始屈服极限

(Edited by Chao WANG)